Journal of Hazardous Materials 474 (2024) 134773

Contents lists available at ScienceDirect

Journal of Hazardous Materials

journal homepage: www.elsevier.com/locate/jhazmat

Cadmium bioaccumulation dynamics during amphibian development and metamorphosis

Chantal Lanctôt[a,*,1], Paul Callaghan[b], Tom Cresswell[b]

[a] Australian Rivers Institute, and School of Environment and Science, Griffith University, Gold Coast, QLD 4222, Australia
[b] ANSTO, Locked Bag 2001, Kirrawee DC, NSW 2232, Australia

HIGHLIGHTS

- Animals exposed at the onset of metamorphic climax retained less Cd than larvae.
- Larvae (Gosner stages 27, 32, and 37) accumulated Cd mainly through their gut.
- Metamorphs (stage 42) accumulated Cd predominantly through their skin and gills.
- The fate of tissue burdens during depuration is stage- and tissue-dependant.
- Cd biodistribution patterns relate to the fate of tissues during metamorphosis.

GRAPHICAL ABSTRACT

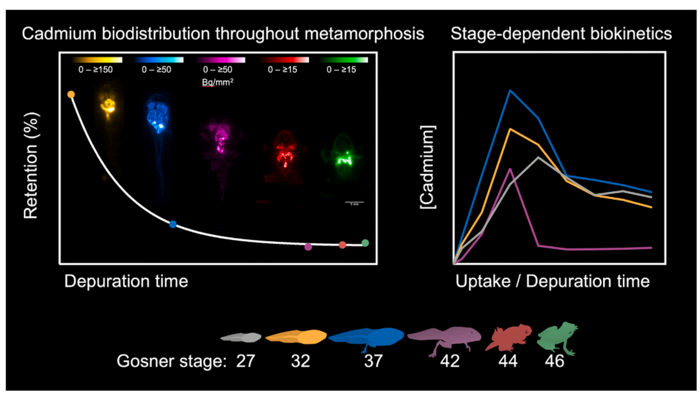

ARTICLE INFO

Keywords:
Metal
Toxicokinetics
Biodistribution
Anuran
Radiotracing

ABSTRACT

Cadmium pollution poses a significant threat to aquatic ecosystems due to its propensity to bioaccumulate and cause toxicity. This study assessed the complex dynamics of cadmium uptake, accumulation and distribution across anuran development to provide new insights into the fate of cadmium burdens during metamorphosis and compare the susceptibility of different life stages to cadmium accumulation. Tadpoles of various developmental stages were exposed to dissolved 109-cadmium and depurated in clean water in a series of experiments. Temporal changes in whole-body and tissue concentrations were analysed using gamma spectroscopy, and anatomical distributions were visualised using autoradiography. Results showed that animals exposed at the onset of metamorphic climax (forelimb emergence) retained significantly less cadmium than animals exposed through larval stages. After exposure, cadmium partitioned predominantly in the skin, gills and remains of metamorphs, whereas larvae accumulated cadmium predominately through their gut. This shows a shift in the primary route of uptake at the onset of climax, which relates to the structural and functional changes of uptake sites through metamorphosis. During climax, some cadmium was redistributed in tissues developing de novo,

* Corresponding author.
E-mail address: c.lanctot@griffith.edu.au (C. Lanctôt).
[1] Current address: Australian Rivers Institute and School of Environment and Science, Griffith University, Gold Coast, Queensland, 4222 Australia.

https://doi.org/10.1016/j.jhazmat.2024.134773
Received 18 April 2024; Received in revised form 28 May 2024; Accepted 29 May 2024
Available online 31 May 2024
0304-3894/

such as the forelimbs, and concentrated in the regressing tail. Our findings highlight the need for stage-specific considerations in assessing exposure risks.

1. Introduction

Metal pollution poses an important threat to aquatic ecosystems due to the persistence and bioaccumulative nature of many toxic elements [1]. Amphibians may be particularly vulnerable to metal uptake, owing to their capacity to absorb dissolved ions through multiple pathways, including their permeable skin, respiratory surfaces, and gastrointestinal tract. While metals accumulated during larval stages are known to persist and even concentrate in amphibians throughout metamorphosis (reviewed by [2]), the fate of metals accumulated in transient and changing tissues during the final energy-intensive stages of metamorphosis (i.e., metamorphic climax) remains poorly understood.

During metamorphosis, amphibians undergo extensive morphological and physiological transformations, including the regression and remodelling of most tissues and organs [3]. These drastic changes can lead to the mobilisation, transference and bioamplification of contaminants burden, which can influence their toxicity during vulnerable life stages [2,4,5]. Our earlier work showed tissue-specific changes in selenium burdens throughout anuran development, including the transference of selenium in developing tissues, such as the limbs, and concentration in the eyes and liver [6]. While that study offers valuable insights into the toxicity implications of selenium transference and concentration during amphibian metamorphosis, further research is warranted to assess the fate of other toxic elements during vulnerable amphibian life stages.

This study focused on cadmium (Cd), a non-essential element of major environmental concern due to its persistence, toxicity and propensity to accumulate in biota [7]. Cadmium pollution primarily stems from industrial activities such as mineral mining, coal combustion, and the manufacturing of various products like nickel-cadmium batteries and pigments [1]. Aquatic habitats downstream of these industries can often exceed water quality guidelines [8-10] by several orders of magnitude, especially in heavily polluted systems [11-13]. For example, Cd concentrations were reported to range between 0.003–13,700 μg/L in a recent global evaluation of metal pollution in surface waters [14], with the average Cd concentration (181 μg/L) far exceeding the Australian and New Zealand [15] freshwater guideline and exposure concentration used in this study (0.5 μg Cd/L). Aquatic Cd concentrations above protection guidelines have been found to adversely affect amphibians by causing mortality, malformations, endocrine disruption, and altering larval growth, development and metabolic processes [16-19]. Importantly, Cd accumulated during larval stages is largely retained during metamorphosis and represents an important pathway of Cd transference between aquatic and terrestrial ecosystems [20,21]. While the toxicity and bioaccumulation of Cd are relatively well-characterised in larval amphibians, little is known about how the morphological and physiological changes associated with metamorphosis influence the uptake, elimination, and biodistribution of this metal.

We investigated the complex dynamics of Cd biodistribution and biokinetics across anuran tadpole development to provide new insights into the fate of Cd burdens during metamorphosis and to determine the developmental period most susceptible to Cd accumulation. Specifically, we assessed spatial and temporal changes in Cd burdens throughout metamorphosis using live animal radiotracing, autoradiography and excised tissue analysis, and compared toxicokinetics across different developmental stages.

2. Materials and methods

2.1. Animals

Eggs of the Australian striped marsh frog (*Limnodynastes peronii*) were collected during spring (March 2019) in Elanora, Queensland, Australia, and transported to a temperature- and light-controlled laboratory where they were slowly acclimated to laboratory water and conditions (photoperiod = 12:12 h light/dark). Tadpoles were housed in an automated re-circulating tank system (ZebTEC, Techniplast) containing moderately hard water prior to experiments (87 mg/L $CaCO_3$). Water physicochemical parameters were monitored daily and were as follows during rearing: temperature = 27.5 ± 0.8 °C, pH = 7.6 ± 0.1, dissolved oxygen (DO) = 93 ± 4 %, and electrical conductivity (EC) = 311 ± 76 μS/cm. Tadpoles were fed Sera Micron fry food (Sera, Heinsberg, Germany) ad libitum, and survival was monitored twice daily. Methods were approved by the Griffith University and ANSTO Animal Care and Ethics Committees (projects ENV/03/17/AEC and P315, respectively; proof of approval is available upon request) and adhered to the Australian Code for the Care and Use of Animals for Scientific Purposes.

2.2. Cadmium analysis

The ^{109}Cd radioisotope stock ($^{109}CdCl_2$ dissolved in 0.1 M HCl, $t_{1/2}$ = 462.6 days) was obtained from Eckert & Ziegler Isotope Products Inc., Valencia, CA. Exposure concentrations were verified by inductively coupled plasma mass spectrometry (ICP-MS; Varian 820MS Quadropole). All samples were run with internal standard correction for matrix and drift correction), and certified reference material (DORM-4 and DOLT-5, National Research Council Canada) samples were analysed to verify the accuracy of the analysis (Recovery = 100.4 ± 6.5 % of the certified value).

The ^{109}Cd activity of the stock was verified using a coaxial high-purity germanium (HPGe) detector (ORTEC) connected to a gamma spectrometer (ORTEC) and spectrum analysis software on a PC. The radioactivity of samples was determined against standards (Eckert & Zeigler, California) in the same geometry (10 mL in 20 mL vial) [22]. All measurements were corrected for background radiation and physical decay. The specific activity of the ^{109}Cd stock was calculated from analytical results (i.e., Bq ^{109}Cd activity per g total Cd).

The radioactivity of ^{109}Cd in experimental samples (water, whole tadpoles, dissected tissues, and standards) in 5 mL glass tubes was determined using an automated gamma counter (Wallac Wizard 1470). The counts from each sample were standardised using geometrically matched in-house liquid standards to provide activity concentrations (Bq/mL) for each sample, as per Lanctôt et al. [23]. To assess the possible influence of minor tadpole movements during live animal radioanalysis, four tadpoles were repeatedly radioanalysed three times (60 s each) to determine the variability between measurements. The relative standard deviation for the radioanalysis procedure was 3 ± 0.02 % and was deemed acceptable. All measurements were corrected for background radiation and physical decay.

2.3. Experiment 1: Changes in whole-body and tissue Cd burdens during metamorphosis

Forty-five Gosner stage 29 (Gs; [24]) tadpoles were exposed individually in square 1.1 L polypropylene containers (1 per container), each containing 400 mL of moderately hard water (MHW; 87 mg/L $CaCO_3$; [25] spiked with ^{109}Cd (501 kBq/L), equivalent to 0.5 μg total Cd/L (nominal). The estimated radiation dose resulting from exposure to this concentration of ^{109}Cd in solution is nearly two orders of magnitude lower than the LD_{50} reported for tadpoles and, therefore, unlikely to influence the results (as described in an earlier study on *L. peronii*; [23]). Four tadpoles were similarly transferred to individual containers with control water (400 mL isotope-free MHW) and subjected to the same handling as the Cd-exposed group. Control animals were reared until the completion of the experiment and served to compare tadpole development over time. The nominal Cd concentration was selected based on the Australian trigger value for the protection of 95 % of freshwater species (corrected for hardness level; [15]). Tadpoles were exposed for nine days, during which exposure solutions were entirely renewed every three days. On day nine, tadpoles were transferred to clean containers with 1000 mL control water for twenty-six days of depuration. Water was renewed daily for the first three days of depuration and every three days thereafter. Aeration was provided in each container. Tadpoles were monitored for survival and development, and fed equal amounts of Sera Micron daily (5 % of body weight/day).

Water samples were collected from four randomly selected replicates before and after water renewals and analysed for total and dissolved (0.45 μm filtered) ^{109}Cd activity. Throughout the exposure period, total and dissolved Cd concentrations were equivalent to 0.60 ± 0.10 μg/L and 0.50 ± 0.08 μg/L, respectively (mean ± SD of 40 measurements; $p < 0.001$; Fig. S1). Although tadpoles were mainly exposed to dissolved Cd (> 0.45 μm filtered), a small proportion was also bound to food or particulate matter (approximately 17 %) as animals were fed within the exposure water. Concentrations fluctuated by 11–28 % (total Cd) and 5–21 % (dissolved Cd) between water changes (average of fresh treatment and aged water) ($p < 0.001$). Measured total and dissolved Cd concentrations of fresh exposure solutions were 0.70 ± 0.03 μg/L and 0.55 ± 0.06 μg/L, respectively. Concentrations were < 0.02 μg Cd/L throughout the depuration phase.

Physicochemical parameters were measured in a subset of replicates throughout the experiment (before and after water renewals) and were (average ± SD of 65–76 measurements): pH = 7.9 ± 0.3, temperature = 26 °C ± 1.0, DO = 87 ± 13 %, EC = 323 ± 11 μS/cm. Ammonia concentrations were determined in randomly selected replicates throughout the experiment with a commercially available semiquantitative test kit (Aquasonic Pty Ltd, Australia).

Seven Cd-exposed tadpoles were sampled at five developmental stages (Gs 32, 37, 42, 44, and 46) on days 0, 9, 21, 24, and 26 of depuration, respectively. Each tadpole was rinsed four times in fresh control water (isotope-free) to remove any loosely adsorbed Cd [22] and euthanised by immersion in 3-aminobenzoic acid ethyl ester (MS222; Sigma Aldrich) dissolved in water and buffered with sodium bicarbonate. Euthanised tadpoles were rinsed with reverse osmosis (RO) water and blotted dry on lint-free tissues (Kimwipes, Kimberly-Clark, Australia). Tadpoles were then individually radioanalysed in 5 mL tubes to determine whole-body ^{109}Cd activity. Morphometric measurements (snout−vent length (SVL), total length, weight) were taken to calculate condition factors ($K = [\text{weight}/\text{SVL}^3] \times 100$).

Following whole-body radioanalysis at each time point, four Cd-exposed tadpoles (of the seven sampled per stage) were dissected for gut, gall bladder, liver, mesonephros, lungs, limbs, gills, eyes, brain, tail, skin, fat bodies and remains (i.e., all other tissues). Tools were cleaned thoroughly using RO water and ethanol between each tissue and animal. Tissues were rinsed with RO water, blotted dry on a lint-free tissue, weighed, dried at 60 °C (>18 h) and re-weighed to obtain dry weights (dw).

Three of the seven tadpoles sampled at each time point were embedded in an inert resin (Cryomatrix, Thermo Fisher Scientific, Australia), frozen in liquid nitrogen-cooled isopentane, and stored at −80 °C [26]. Triplicate ventral sections (30 μm) were collected from the frozen blocks at 4–5 positions targeting organs of interest using a cryomicrotome (Cryostat Leica CM3050 S, Leica Biosystems), and thaw mounted onto glass slides. A digital photo of the block face (i.e., sample block facing the cryomicrotome blade) was taken for each section (Canon EOS 500 D) to aid organ identification. Slides were dehydrated on a slide warmer at 37 °C for 15 min and exposed to a phosphor plate (BAS-SR 2040) for 2–16 days, and plates were subsequently visualised using a GE Typhoon FLA 7000. Standards for ^{109}Cd autoradiography were created in-house to allow for the quantification of the autoradiographs (see supplementary methods S1). Autoradiography images were analysed using Fiji (ImageJ) to provide additional information on the spatial partitioning of Cd accumulation in tadpoles at different stages of development.

2.4. Experiment 2: Stage-specific Cd toxicokinetics

Tadpoles of Gs 27, 32, 37, and 42 (n = 8 per stage) were individually transferred to polypropylene containers containing 400 mL of ^{109}Cd (501 kBq/L) equivalent to 0.5 μg total Cd/L (nominal). Each exposure chamber contained an internal polypropylene basket to facilitate the handling of the animals. Aeration was provided in each container. Animals were transferred at 5-minute intervals to account for the time required for live radioanalysis procedures. Tadpoles were exposed for two days, after which four tadpoles per stage were sampled (described below). The remaining four animals per stage were transferred to clean exposure chambers with 1000 mL of control water for a 5-day depuration period, during which water was renewed daily. Tadpoles were monitored and fed as described for experiment 1 (Section 2.3), except that tadpoles were not fed during the 2-day exposure. No food was provided to Gs 42–46 animals as animals fast during metamorphic climax. Water physicochemical parameters measured throughout the experiment were (average ± SD): pH = 7.9 ± 0.3, temperature = 26 °C ± 0.9, DO = 89 ± 13 %, EC = 315 ± 11 μS/cm. Water samples were collected daily before and after water renewals and radioanalyzed for total and dissolved ^{109}Cd activity. Measured Cd concentrations were 0.38 ± 0.06 μg/L (average ± SD of 88 measurements) in solution throughout the 2-d exposure period (Fig. S2). Concentrations decreased by 18–22 % between the start and end of the exposure phase ($p < 0.001$). No differences between total and dissolved concentrations or between sub-experiments (different stages) were observed ($p > 0.05$) – this differed from experiment 1 (Section 2.3), where animals were fed during exposure due to the longer exposure period. Measured concentrations of fresh exposure solutions were 0.41 ± 0.02 μg/L (total Cd) and 0.42 ± 0.06 μg/L (dissolved Cd). Total and dissolved Cd concentrations were ≦ 0.02 μg/L throughout the depuration phase.

Tadpoles of each stage were radioanalysed after 6, 24, and 48 h during the exposure period (n = 8) and every 24 h during the depuration phase (n = 4). Tadpoles were removed from their respective exposure chambers using the internal baskets and consecutively transferred between four different rinse solutions (250 mL control water) for 10 s each to remove any loosely adsorbed radionuclides. Following rinsing, each tadpole was transferred to a 5 mL glass vial containing 1 mL of non-active control water and weighed (each vial was pre-weighed with water to estimate tadpole weight). Vials were individually transferred to the gamma counter (Wallac Wizard 1470) for 30–60 s to determine ^{109}Cd activity. Tadpoles were then returned to their respective chambers.

At the end of both the exposure (day 2) and depuration phase (day 7), four tadpoles per stage were euthanised by immersion in MS222. Euthanised tadpoles were rinsed with RO water, blotted dry on a lint-free tissue, staged, and measured for SVL (mm), tail length (mm), and wet weight (mg). Tadpoles of stages Gs 27, 32, 37, and 42 at the start of the exposures reached stages 30 ± 1, 34 ± 1, 39, and 46, respectively, at the end of the seven-day experiments. Gut, liver, mesonephros, lungs, gills, skin, and remains were dissected from each tadpole, weighed, dried, and analysed as described for experiment 1 (Section 2.3).

2.5. Statistical analysis

Data were first analysed for normality and homogeneity of variance in all cases. Percentage data were arcsine square root transformed prior to analysis. The significance level was set at $\alpha \leq 0.05$ for all tests. Differences in aqueous Cd concentrations (total and dissolved) over time were analysed using a three-way ANOVA with time, replicate, and type (total vs. dissolved) as factors. Analysis was performed using SPSS v27. All other analyses were performed using GraphPad Prism v10.0.0.

Changes in whole-body Cd concentrations throughout tadpole development and metamorphosis obtained in experiment 1 (Section 2.3) were analysed using repeated measures one-way ANOVAs followed by multiple comparisons test. This test was also used to test differences in Cd tissue concentrations, total burdens and biodistribution (non-parametric tests were used when parametric assumptions were not met). Biodistribution data were arcsine square root transformed before analysis. Retention efficiencies (RE, %) were calculated by fitting a first-order decay model: $RE_t = RE_0 \times e^{-ke \times t}$, where RE is the percentage of Cd remaining in the tadpoles or organs at time t (d), and k_e (d $^{-1}$) is the depuration rate constant for Cd loss and used the corresponding *y*-intercept to estimate Cd retention efficiency [27,28]. Depuration half-lives ($t_{1/2}$, d) are calculated on the exponential part of the depuration curve using $t_{1/2} = \ln(2)/k_e$.

Differences in size (i.e., SVL and weight), *K*, development, Cd burdens, and biodistribution of animals in experiment 2 (Section 2.4.) were analysed using two-way repeated measures ANOVAs with developmental stage (Gs) and time as factors. The influx rates (I_u, ng/g/d) were calculated using the slope of the linear regression line of Cd accumulation during the first two days of exposure with the intercepts set at zero [29]. The I_u calculated includes efflux processes likely occurring during the exposure phase, which is noteworthy as efflux processes may vary between the developmental stages being compared. Differences in Cd I_u and retention (%) between developmental stages were analysed using one-way ANOVAs. Mixed-effect models (REML) were used to test differences in Cd burdens and retention between the tissues and stages. Tukey HSD post hoc comparisons were used to determine specific differences between tissues.

3. Results and discussion

3.1. Cadmium retention kinetics throughout tadpole metamorphosis

After nine days of exposure to 0.50 ± 0.08 μg Cd/L in experiment 1, tadpoles bioaccumulated 359 ± 50 ng Cd/g ww (Fig. 1). Once transferred to clean water, whole-body Cd decreased significantly over time ($F_{(1.3,8)} = 194$, $p < 0.0001$), following an exponential decay pattern (Fig. 1 and Table S1). A steady state was reached after 21 days of depuration, with only 11 % of the initial Cd (45 ± 3 ng Cd/g ww) retained until the end of the experiment and completion of metamorphosis. The initial rapid loss reflects the initial gut passage time, followed by a slower elimination of accumulated Cd [30,23,31], with no significant change in whole-body concentrations during the final stages of metamorphosis, known as the metamorphic climax (Gs 42–46). Our findings are consistent with several studies showing that tadpoles exposed to Cd-contamination, including coal combustion waste, retain Cd burdens post-metamorphosis [32-34,20]. In these studies, animals typically retained approximately 70 % of Cd after completing metamorphosis when not subjected to a depuration period (reviewed by [2]).

Most anuran species stop feeding during metamorphic climax when the oral structures and gastrointestinal tract undergo major changes to accommodate the dietary shift from predominantly omnivorous tadpoles to carnivorous adults. As such, anurans often experience a considerable loss in body mass and reduced condition factor (*K*) during this energy-intensive period. In this study, animals lost an average of 30 % of their body mass as they progressed through metamorphic climax, with a 50 % reduction in *K* (Fig. S3 and Fig. S4). To account for the non-linear growth pattern and potential for bioamplification resulting from the rapid weight loss, changes in total Cd burdens (total Cd per tadpole) were also assessed (Fig. S5) and compared with whole-body concentrations (Cd per unit of mass). Whole-body Cd burdens showed a less rapid decrease and higher retention than kinetics based on Cd concentrations (RE = 19 % vs. 11 %; Table S1), showing the influence of animal growth and development. Understanding the retention of elements through metamorphosis is important as amphibians are known to transfer nutrients and contaminants from aquatic to terrestrial ecosystems [21,35], potentially providing toxic elements to terrestrial predators.

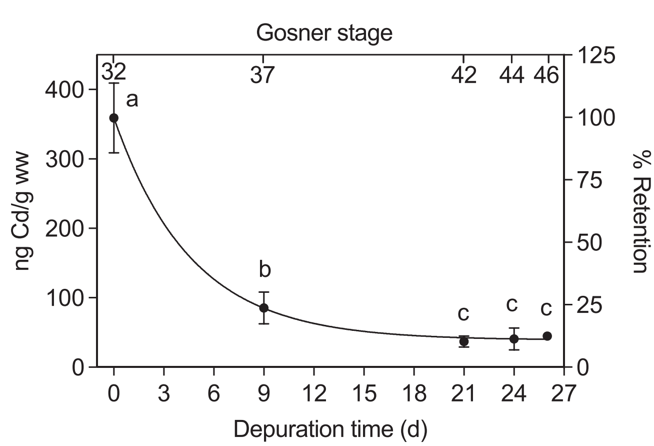

Fig. 1. Cadmium concentration (ng Cd/g wet weight; left) and retention (%; right) in whole tadpoles exposed for nine days and sampled at different developmental stages [24] throughout 26 days of depuration in control water. Values are means ± SD (n = 7). The line shows the best-fit one-phase exponential decay ($R^2 = 0.96$). Letters indicate significant differences in Cd concentrations among developmental stages, based on Holm-Šídák's multiple comparisons test with α = 0.05.

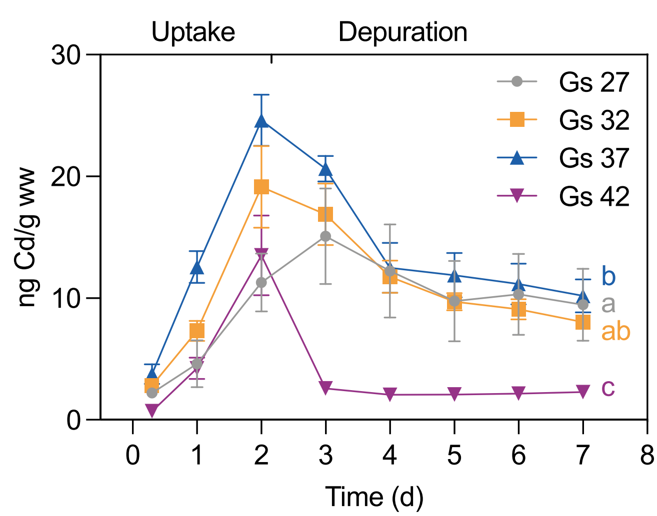

Fig. 2. Cadmium concentration (ng Cd/g wet weight) in whole tadpoles exposed for two days (uptake; n = 8) at different developmental stages (Gs, Gosner [24]) followed by five days in clean water (deputation; n = 4). Values are means ± SE. Letters indicate significant differences in Cd concentrations among developmental stages, based on Tukey's multiple comparisons test with α = 0.05.

3.2. Stage-dependent bioaccumulation kinetics

Our findings showed that Cd uptake and depuration kinetics differed significantly across tadpole development and metamorphosis (Fig. 2; Experiment 2). Accumulation and depuration patterns were found to relate to the morphological and physiological changes associated with growth early in development and metamorphosis later in development. More specifically, the size of larval stages (Gs 27, 32 and 37) gradually increased throughout the experiment, whereas the weight, total length and condition factor of metamorphs decreased as the animals progressed through metamorphosis (Gs 42–46; Fig. S4). Prometamorphic tadpoles (Gs 37), the largest of the larval stages assessed, displayed the highest Cd influx rates (2–3 times higher than premetamorphic Gs 27 tadpoles), which resulted in the highest whole-body concentrations (Fig. 2) and total body burdens (Fig. S6a) at the end of the 2-day exposure. Similar stage-dependent increases in Cd uptake have been reported in earlier anuran life stages exposed as embryos, hatchlings and premetamorphic larvae [36]. The stage-dependent increase in Cd uptake in the larval stages could be explained by the increased ingestion rate, metabolic demands and intestine surface area reported with increased body mass [37,38].

The reduced Cd influx observed in metamorphic animals (47 % decrease between Gs 37 and Gs 42), on the other hand, likely relates to the drastic restructuring of uptake sites, including the remodelling of the skin and gastrointestinal tract and regression of internal gills during the final stages of metamorphosis when anurans also cease feeding [39]. These changes may result in Cd elimination exceeding uptake rates, resulting in lower accumulation in metamorphs [33]. Likewise, animals exposed at the onset of metamorphic climax depurated three times more Cd during the first day of depuration compared to the larval stages (Fig. S6b) and overall retained half that of the earlier stages after five days of depuration (26 % vs 42–63 %; $F_{(3,\ 12)} = 14.8$, $p = 0.0002$; Fig. 3b). Though research comparing the toxicokinetics of contaminants among anuran life stages is limited, the higher Cd elimination observed during metamorphic climax aligns with the higher polychlorinated biphenyl (PCB) elimination rates reported in leopard frog (*Lithobates pipiens*) and green frog (*Lithobates clamitans*) metamorphs compared to tadpoles and adults [40]. These findings relate to the transformation and resorption of larval tissues and organs during metamorphic climax [41], when contaminant burdens may be mobilised and eliminated [6], as further described in Sections 3.3 and 3.4.

3.3. Cadmium biodistribution and redistribution during metamorphosis

Our findings demonstrate the complex and dynamic changes in Cd biodistribution during tadpole metamorphosis (Fig. 4). The changes reflect three transformative processes that relate to the metamorphic fate of tissues and organs: remodelling, resorption (tissue breakdown), and de novo development [42,43]. These include larva-to-adult tissues, such as the gut, liver and body skin, that persist through metamorphosis but undergo significant structural and functional transformations, larva-specific tissues, such as the gills and tail, that regress during metamorphosis and are not present in adults, and adult-specific tissues, such as the forelimbs, that develop during metamorphosis.

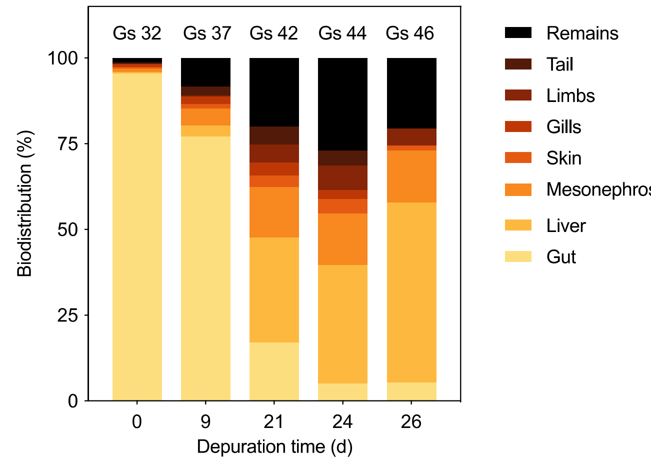

Fig. 4. Average proportion (%) of Cd in tadpole tissues (μg Cd/organ) relative to total body burdens (i.e., the sum of all tissues) in animals sampled at different developmental stages [24] over a 26-day depuration phase following a 9-day Cd exposure (n = 4).

After a 9-day exposure, the majority of Cd was initially located within the gut of tadpoles (~95 %), with the remainder distributed in the mesonephros, gills and remains (~1 % each), as well as in the liver, body skin and tail (~0.5 % each; Fig. 4). This confirms that tadpoles mainly absorb dissolved and particle-bound Cd through their gut. It should be noted that the digestive tracts of animals were not purged prior to analysis, so whole guts sampled immediately post-exposure (day 9) include both Cd bioaccumulated within the gut lining and unabsorbed Cd in the gut lumen. Nevertheless, autoradiographs show higher concentrations in the gut lining than the gut lumen throughout development (Fig. 5), confirming uptake through the digestive tract. Our findings are consistent with those reported for estuarine and marine fish, which, akin to tadpoles, predominantly accumulate Cd via their digestive tract [44, 45], but contrast freshwater fish that accumulate dissolved Cd

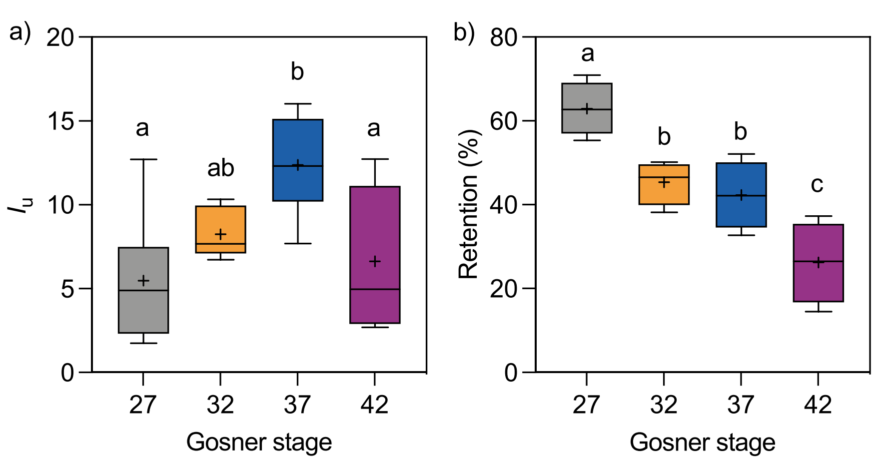

Fig. 3. (a) Cadmium influx rates (I_u, ng/g/d) over a 2-day exposure (n = 8) and (b) retention (%) following five days in clean water (deputation; n = 4) in tadpoles exposed at different stages of development [24] in Experiment 2. Boxplots show interquartile range (column), median (horizontal line), minimum and maximum values (whiskers), and mean (+). Letters indicate significant differences among developmental stages ($p < 0.05$; Tukey's posthoc test).

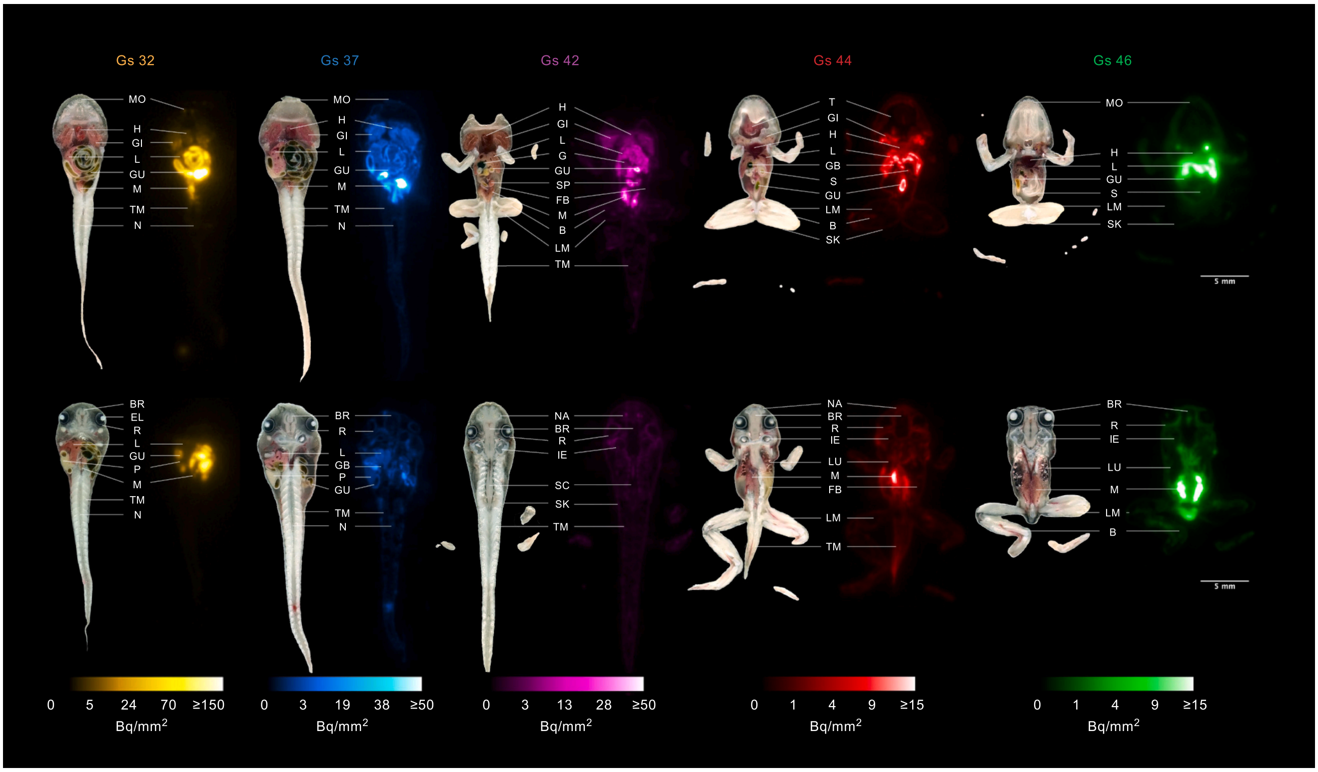

Fig. 5. Digital autoradiographic phosphor image and optical image of block face (right and left, respectively, in each panel) showing 109-Cd distribution in ventral (top row) and dorsal (bottom row) sections of tadpole at Gosner stage (Gs) 32 (yellow), Gs 37 (blue), Gs 42 (magenta), Gs 44 (red), and 46 (green), sampled after 0, 9, 21, 24, and 26 days of depuration in clean water, respectively. B, bone; BR, brain; EL, eye lens; FB, fat bodies; G, gallbladder; GI, internal gills; GU, gut; H, heart; IE, inner ear; L, liver; LM, limb muscle; LU, lung; M, mesonephros; MO, mouth; NA, nare; N, notochord; P, pancreas; R, retina; S, stomach; SC, spinal cord; SK, skin; SP, spleen; TM, tail muscle. Scale bar applies to all panels.

predominantly through their gills [46,47]. The discrepancy relates to the fact that tadpoles, like estuarine and marine fish, ingest water for osmoregulation, thereby accumulating dissolved ions through their gut.

While the gut lining can also serve as a storage site for Cd, as shown in the autoradiographs (Fig. 5), it is primarily involved in the elimination and redistribution of Cd. This is reflected in our depuration kinetics results that show a substantial decrease in gut Cd over time, with only 1.3 ± 0.5 % of the initial Cd retained in the digestive tract at the end of metamorphosis ($p < 0.0001$; Fig. 6a, Fig. S7). As described for the whole-body kinetics (Section 3.1), the initial rapid loss of Cd in the gut during depuration reflects the initial gut passage time (typically <14 h in tadpoles [30,48], which is followed by a slower elimination and redistribution of accumulated Cd to other tissues [49-51]. During metamorphic climax, however, the gastrointestinal tract undergoes drastic structural and functional transformations, whereby primary (larval) epithelial cells are replaced by secondary (adult) epithelial cells to form a more complex multi-folded epithelium and substantially shorter intestine (60–90 % length reduction) [3,52,53]. The 12-fold decreased Cd concentration observed during climax ($p = 0.04$; Fig. 6a) reflects these transformations [43]. Despite the low proportion of Cd retained in the gut, the elevated Cd at the end of the exposure aligns with reports of Cd-induced gut toxicity. For example, studies have reported intestinal histopathological damage and altered gut microbial communities in Cd-exposed tadpoles, which can lead to longer-term health effects and increased risk of disease [54,55].

The gills and semi-permeable skin of tadpoles also contributed to Cd uptake, though significantly less Cd was partitioned to those tissues at the end of the exposure (Figs. 4 and 5). Total Cd burdens in the gills and body skin were largely retained until the onset of metamorphic climax, after which a two-fold decrease was observed (Fig. S8). As reported for the gut, the reduced tissue burdens during climax align with tissue-specific metamorphic transformations. During climax, the internal gills are regressed with only a small fraction of the tissue visible post-metamorphosis [56] (Fig. 5), which explains the observed decrease in gill Cd. Conversely, the metamorphic fate and cellular composition of skin cells are region-specific. Namely, the tail skin regresses through programmed cell death (larva-specific), whereas the body skin is transformed into adult-type skin (larvae-to-adult) [43,57]. As such, it is important to note that this study only assessed a sub-section of the dorsal (body) skin. The restructuring of body skin cells involves the apoptosis of some larval cells and the proliferation of others into more complex adult skin that resembles mammalian skin structure [58], which relates to the decreasing Cd concentration during climax ($p = 0.04$; Fig. 6b). Nevertheless, given the known differences in the metamorphic fate of skin cells, further investigations are needed to determine the fate of Cd in other skin regions.

Like the internal gills, the tadpole tail regresses rapidly during metamorphic climax through apoptosis processes [41]. In the tail, Cd partitioned primarily in the tail skin, vasculature and muscle, with minimal Cd accumulation in the notochord and spinal cord (though elevated Cd was found within the central canal of the spinal cord in the body sections; Fig. 5). Cadmium concentrations increased two-fold in the regressing tail during metamorphosis ($p = 0.01$; Fig. 6c), and autoradiographs showed higher Cd concentrations in the distal part of the tail (Fig. 5). The concentration of Cd relates to the three-fold reduction in tail mass (dw) observed between Gs 42 and 44 and biochemical changes reported in the regressing tail, including tissue acidification and dehydration [43]. Concentrated tissue burdens can impair tissue structure and physiology by inducing cellular and molecular stress responses [59], which can increase the susceptibility of metamorphs to stressors during an already vulnerable life stage [60].

Detoxification organs such as the liver and mesonephros retained the

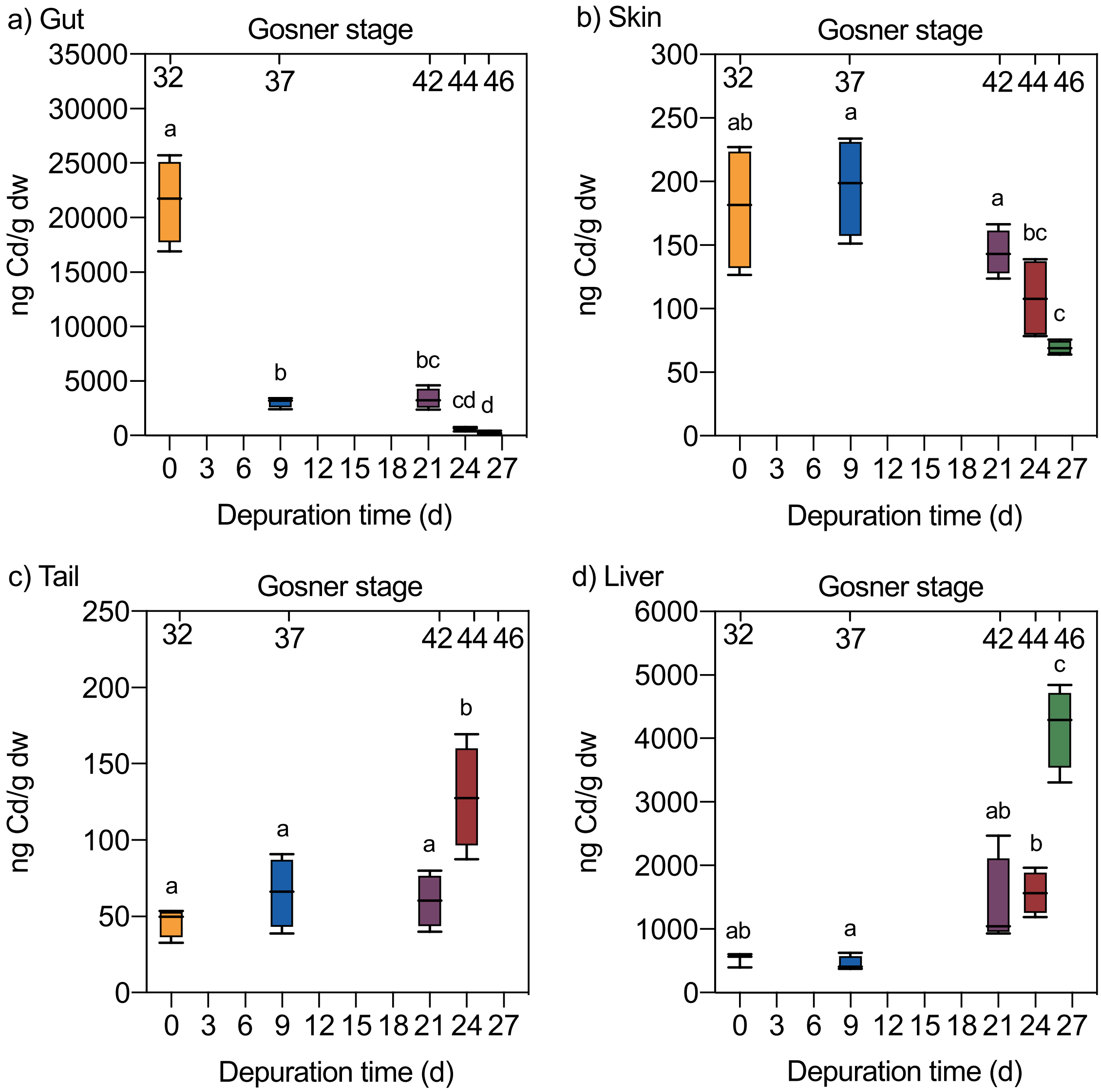

Fig. 6. Cadmium concentration (ng Cd/ g dry weight) in the gut, body skin, liver and tail of tadpoles exposed for nine days and sampled at different developmental stages throughout 26 days of depuration in clean water (Experiment 1). Boxplots show interquartile range (column), median (horizontal line), and minimum and maximum values (whiskers) of 3 – 4 replicates. Letters indicate significant differences between developmental stages (α = 0.05).

highest proportion of whole-body Cd (Fig. 4), which related to their role in metal sequestration, detoxification and excretion, mainly through the induction of metal-binding metallothioneins [61,62]. Tadpoles accumulated 524 ± 110 ng Cd/g dw in the liver at the end of the 9-day exposure, which progressively increased through tadpole development (1372 ± 737 ng Cd/g dw at Gs 42) and metamorphosis (4184 ± 640 ng Cd/g dw at Gs 46; $F_{(4,\ 14)} = 0.38$, $p < 0.0001$; Fig. 6d). This trend aligns with a similar study that reported a 6-fold increase in hepatic Cd during metamorphosis in *Xenopus* exposed to 30 µg Cd/L for 12 days, followed by a depuration in clean water until the completion of metamorphosis [63]. The observed bioamplification was hypothesised to result from the substantial decrease in liver mass between stages 42 and 46, consistent with the 50 % decrease in liver dry mass in this study (75 % decrease in liver wet weight). Accumulation of Cd in hepatic and renal tissues may have important consequences for metamorphosing amphibians as it has been linked to a range of hepatotoxic and nephrotoxic effects, such as necrosis, increased and enlarged Kupffer cells and histopathological lesions [64]. The shift of Cd from the digestive tract to the liver and kidneys is in line with several other studies [44,65], though the relative importance of the target organs in sequestering Cd is known to vary between species, route of uptake and exposure concentration ([66,67]; Kraal et al., 1995b).

The increased proportion of Cd in tissues developing de novo, such as the limbs, throughout the depuration phase provides evidence of Cd transference, as no new Cd was administered during the depuration phase. Autoradiographs revealed that Cd was more concentrated in the skin and skeleton (bone and cartilage) of the limbs relative to the muscles (Fig. 5). To our knowledge, this is the first report of Cd accumulation in the skeleton of developing tadpoles, though it has been reported in other vertebrates [68], namely in osteoblastic, cartilaginous and early mineralising areas [69]. The accumulation of Cd in the skeleton may be linked to its similar physicochemical properties to calcium (Ca^{2+}), enabling its uptake via calcium channels [70], and may relate to previously observed delayed skeletal development and reduced ossification rate in tadpoles exposed to high Cd concentrations [19,71,64]. Cadmium-impaired endochondral ossification and skeletal development can severely impact amphibian fitness post-metamorphosis by affecting their jumping performance and movement and, thus, their ability to escape predators, capture prey and find suitable breeding sites [72].

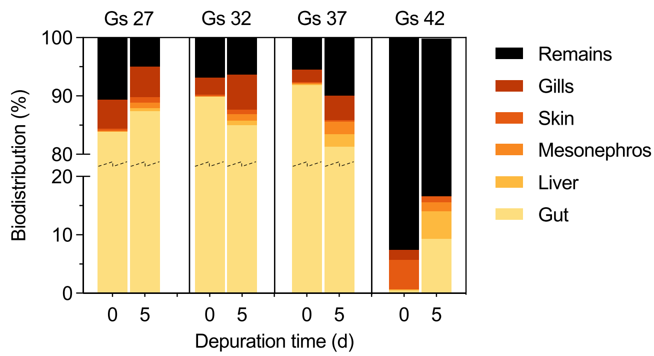

Fig. 7. Average proportion (%) of Cd in tissues (μg Cd/organ) relative to total body concentrations (i.e., sum of all tissues) at the start and end of the 5-day depuration period for each of the developmental stages. Dotted lines indicate a break in the y-axis.

3.4. Stage-dependent absorption and distribution

Comparisons of Cd biodistribution patterns in animals exposed at different life stages showed a shift in the primary route of dissolved Cd uptake at the onset of metamorphic climax (Fig. 7). Specifically, larval stages (Gs 27, 32 and 37) were found to accumulate Cd predominately in the gut > gills > body skin at the end of the uptake period (day 0 of depuration; Fig. 7). Animals exposed at the onset of metamorphic climax (Gs 42), on the other hand, had a higher proportion of Cd in body skin > gill > gut, with the highest proportion of Cd partitioned in the 'remains' consisting of the undissected skin and other tissues.

The elevated Cd concentrations in the gut of larval stages in experiment 2 (Fig. 7) are consistent with the biodistribution results of experiment 1 (Fig. 4) and showed stage-dependent accumulation patterns. Gut Cd concentrations were three times higher in prometamorphic tadpoles (Gs 37) compared to earlier stages at the end of the 2-d uptake period (Fig. 8a). However, Gs 37 tadpoles saw the most significant loss in gut Cd throughout the depuration phase, with only 22 % of Cd retained compared to 64 % in the earlier stages (Fig. S10a). Nevertheless, all larval stages (Gs 27–37) had similar residual gut Cd concentrations after depuration (Fig. 7a). Animals exposed during metamorphic climax, on the other hand, accumulated, on average, 50–150 times less Cd in their gut. The lower accumulation can be attributed to the significant metamorphic transformation of the digestive tract through which the amount, variety and affinities of membrane transporters in the gut are altered [73]. In addition, animals cease feeding during climax, which impairs the absorption of nutrients and contaminants through the gut [39,74]. However, further research is needed to compare Cd uptake via the digestive tract once animals resume feeding post-metamorphosis as the development of digestive structures, including digestive glands and multi-folded secondary epithelium, is likely to influence contaminant uptake [73].

The skin and gills also play a significant role in Cd uptake and were found to display stage-specific accumulation patterns (Fig. 8 and Fig. S10). Metamorphs were found to accumulate 4–7-fold more Cd in their skin than larval stages at the end uptake phase (Fig. 7). However, after five days of depuration, Cd concentrations in the skin of metamorphs decreased by 92 % (Fig. 8e). This is contrary to larval stages that retained and concentrated Cd in their skin during the depuration phase, resulting in a 1.3–2.5-fold increase (Fig. 8e). Although the skin is an important site of Cd accumulation at the onset of metamorphic climax, the extensive metamorphic transformations [75,57,58] significantly alter its capacity to absorb contaminants, leading to reduced cutaneous Cd burdens (as previously described in Section 2.3). Contrary to the skin, gill concentrations were two-fold higher in Gs 37 tadpoles post-exposure compared to other stages. This could be explained by the greater ion

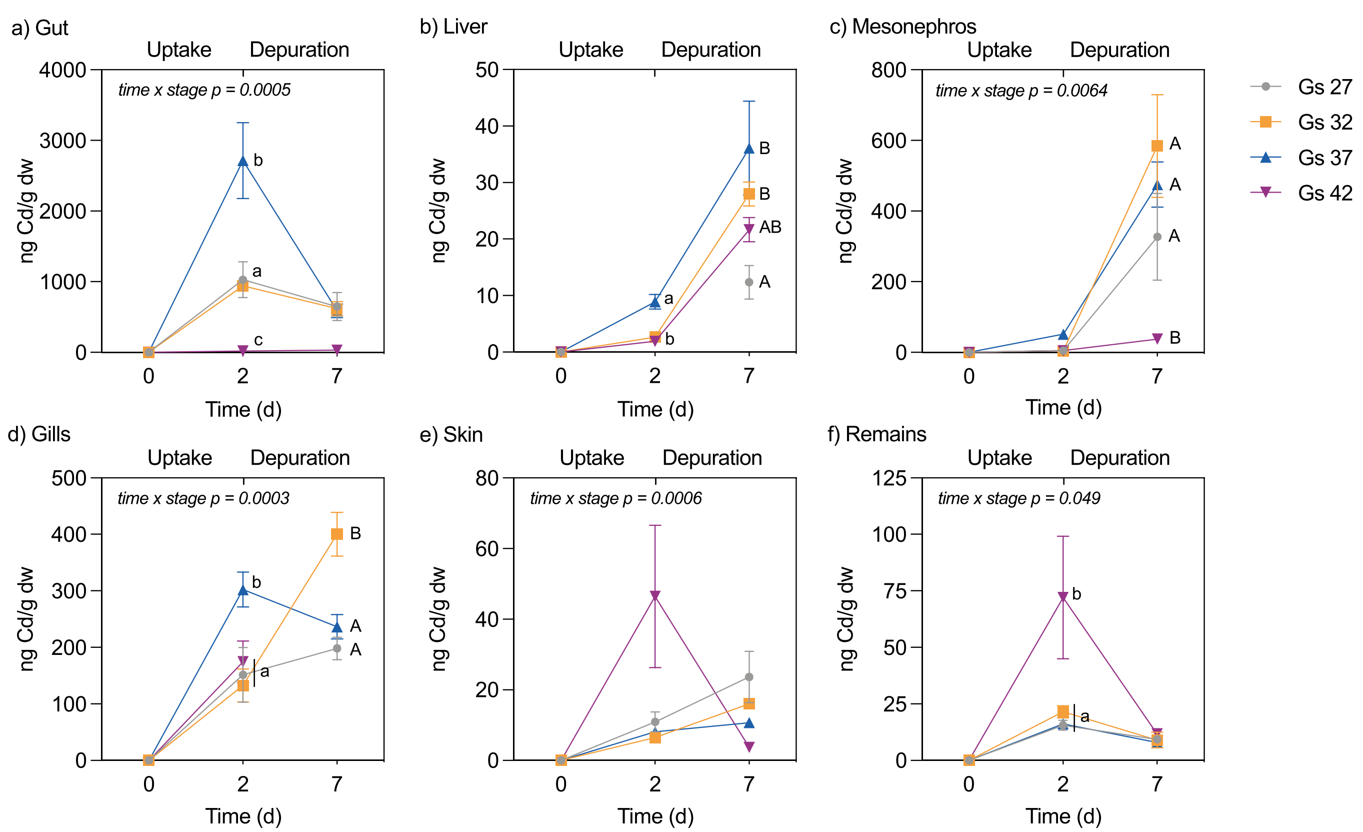

Fig. 8. Tissue Cd concentrations (ng Cd/g dry weight) in tadpoles exposed at different developmental stages (Gs, [24]) for two days (uptake) followed by five days in clean water (deputation). Values are means ± SE (n = 4). Significant interactions between time and developmental stage are indicated in italics ($p < 0.05$; REML). Letters indicate significant differences among developmental stages at each time point ($p < 0.05$; Tukey's posthoc test; day 2, lowercase and day 7, uppercase).

exchange during late larval stages, which is correlated with the increased body and gill mass [37,56]. During metamorphic climax, the tadpole gills regress, resulting in reduced surface area, vasculature and ion transport system [76], which reduces the rate and efficiency of uptake.

Irrespective of the route of uptake and developmental stage, cadmium was found to concentrate in the liver and mesonephros during both the uptake and depuration phases (Fig. 8). In all stages, Cd was more concentrated in the mesonephros than the liver, with 13–16 times higher concentration in the mesonephros of larval stages and twice the concentration in metamorphs at the end of the depuration phase. Although all stages concentrated Cd in the liver and mesonephros, metamorphic animals retained much lower concentrations (9–16 times lower) in their mesonephros at the end of the depuration phase compared to the larval stages. During metamorphic climax, the liver and mesonephros undergo substantial cellular restructuring to accommodate shifts in diet and environment [39,77], which is shown to affect the accumulation and excretion of Cd.

4. Conclusion

This study describes how anuran metamorphosis influences the fate and bioaccumulation dynamics of Cd under environmentally realistic exposure concentrations, highlighting the importance of stage-specific considerations when assessing exposure risks to environmental toxicants. Amphibians, being among the most threatened animal groups, are particularly vulnerable due to their unique physiology, life history, and ecology [78,79]. The shift in the primary route of dissolved Cd uptake and significant changes in Cd tissue burdens observed during metamorphic climax in this study emphasises the need to better understand how the drastic morphological, physiological, and functional transformations associated with metamorphosis influence the bioaccumulation of toxicants. Such knowledge is essential for assessing toxicity risks, informing predictive physiologically-based biokinetic and toxicodynamic models, and developing conservation measures that protect the most vulnerable life stages, as bioaccumulation directly influences the susceptibility of organisms [80,2,81]. For instance, understanding stage-dependent toxicokinetics of Cd in amphibians could help in timing wastewater releases to avoid specific life stages based on seasonal reproductive patterns, particularly in freshwater systems downstream of mining operations where episodic exposures often occur [82]. Furthermore, understanding the retention of chemicals through metamorphosis provides important insights into the transfer of pollutants across ecosystem boundaries through predation and metamorphosis [33].

Environmental implications

Cadmium is classified as a hazardous substance of high priority due to its persistence, toxicity, and tendency to accumulate in living organisms. This research provides new insights into the accumulation dynamics of cadmium during anuran metamorphosis, emphasising the importance of considering development when assessing exposure risks. This is important as amphibians are among the most threatened animal groups and are found to be more vulnerable to some stressors during metamorphic stages. Additionally, our findings highlight the significance of understanding the fate of contaminant burdens through ontogeny, as toxicants can be transferred across ecosystem boundaries through predation and metamorphosis.

CRediT authorship contribution statement

Tom Cresswell: Writing – review & editing, Resources, Methodology, Funding acquisition, Conceptualization. **Chantal M Lanctôt:** Writing – review & editing, Writing – original draft, Visualization, Methodology, Investigation, Funding acquisition, Formal analysis, Data curation, Conceptualization. **Paul Callaghan:** Writing – review & editing, Resources, Investigation, Data curation.

Declaration of Competing Interest

The authors declare the following financial interests/personal relationships which may be considered as potential competing interests: Chantal Lanctot reports equipment, supplies and travel were provided by Australian Nuclear Science and Technology Organisation. Chantal Lanctot reports financial support was provided by Australian Research Council. If there are other authors, they declare that they have no known competing financial interests or personal relationships that could have appeared to influence the work reported in this paper.

Data availability

Data will be made available on request.

Acknowledgements

This study was conducted at the Australian Nuclear Science and Technology Organisation (ANSTO) under research proposal AP11943 and ANSTO Animal Care and Ethics Committee approval P315. CL was supported by an Australian Research Council (ARC) Discovery Early Career Award (DE180101286) funded by the Australian Government. We thank ANSTO staff members Lida Mokhber-Shahin for gamma analyses of standards, Henri Wong for ICP-MS analysis and Charmaine Day for animal support.

Appendix A. Supporting information

Supplementary data associated with this article can be found in the online version at doi:10.1016/j.jhazmat.2024.134773.

References

[1] Tchounwou, P.B., Yedjou, C.G., Patlolla, A.K., Sutton, D.J., 2012. Heavy metal toxicity and the environment. Mol, Clin Environ Toxicol 101, 133–164. https://doi.org/10.1007/978-3-7643-8340-4_6.
[2] Hill, D., Cresswell, T., Bennett, W., Lanctôt, C., 2022. Fate and sublethal effects of metals during amphibian metamorphosis: a systematic review. Crit Rev Environ Sci Technol 52, 4266–4283. https://doi.org/10.1080/10643389.2021.2002117.
[3] Brown, D.D., Cai, L., 2007. Amphibian metamorphosis. Dev Biol 306, 20–33. https://doi.org/10.1016/j.ydbio.2007.03.021.
[4] Humphries, J.E., Lanctôt, C.M., Robert, J., McCallum, H.I., Newell, D.A., Grogan, L. F., 2022. Do immune system changes at metamorphosis predict vulnerability to chytridiomycosis? An update. Dev Comp Immunol 136. https://doi.org/10.1016/j.dci.2022.104510.
[5] Wesner, J., Kraus, J.M., Henry, B., Kerby, J., 2020. Metamorphosis and the impact of contaminants on ecological subsidies. Contam Ecol Subsid 111–125. https://doi.org/10.1007/978-3-030-49480-3_6.
[6] Lanctôt, C., Cresswell, T., Callaghan, P.D., Melvin, S.D., 2017. Bioaccumulation and biodistribution of selenium in metamorphosing tadpoles. Environ Sci Technol 51, 5764–5773. https://doi.org/10.1021/acs.est.7b00300.
[7] McGeer, J.C., Niyogi, S., Scott Smith, D., 2011. Cadmium, in: Fish Physiology. Academic Press, pp. 125–184. https://doi.org/10.1016/S1546–5098(11)31025–4.
[8] ANZG, 2018. Australian and New Zealand Guidelines for Fresh and Marine Water Quality. Canberra, Australia.
[9] UNEP, 2010. Final Review of Scientific Information on Cadmium. UNEP Chemicals Branch,, Geneva, Switzerland.
[10] US EPA, 2016. Aquatic life ambient water quality criteria update for cadmium, EPA-820-R-16–002. Washington, D.C.
[11] Luo, C., Routh, J., Dario, M., Sarkar, S., Wei, L., Luo, D., et al., 2020. Distribution and mobilization of heavy metals at an acid mine drainage affected region in South China, a post-remediation study. Sci Total Environ 724, 138122. https://doi.org/10.1016/j.scitotenv.2020.138122.
[12] Pan, J., Plant, J.A., Voulvoulis, N., Oates, C.J., Ihlenfeld, C., 2010. Cadmium levels in Europe: implications for human health. Environ Geochem Health 32, 1–12. https://doi.org/10.1007/s10653-009-9273-2.
[13] Zhao, X.M., Yao, L.A., Ma, Q.L., Zhou, G.J., Wang, L., Fang, Q.L., et al., 2018. Distribution and ecological risk assessment of cadmium in water and sediment in Longjiang River, China: implication on water quality management after pollution accident. Chemosphere 194, 107–116. https://doi.org/10.1016/j.chemosphere.2017.11.127.

[14] Kumar, V., Parihar, R.D., Sharma, A., Bakshi, P., Sidhu, G.P.S., Bali, A.S., et al., 2019. Global evaluation of heavy metal content in surface water bodies: A meta-analysis using heavy metal pollution indices and multivariate statistical analyses. Chemosphere 236, 124364. https://doi.org/10.1016/j.chemosphere.2019.124364.

[15] ANZECC, ARMCANZ, 2000. Australian and New Zealand Guidelines for Fresh and Marine Water Quality.

[16] Chagas, B.R.C., Utsunomiya, H.S.M., Fernandes, M.N., Carvalho, C.S., 2020. Metabolic responses in bullfrog, *Lithobates catesbeianus* after exposure to zinc, copper and cadmium. Comp Biochem Physiol Part - C: Toxicol Pharmacol 233, 108768. https://doi.org/10.1016/j.cbpc.2020.108768.

[17] Gross, J.A., Chen, T.H., Karasov, W.H., 2007. Lethal and sublethal effects of chronic cadmium exposure on northern leopard frog (*Rana pipiens*) tadpoles. Environ Toxicol Chem 26, 1192–1197. https://doi.org/10.1897/06-479R.1.

[18] James, S.M., Little, E.E., Semlitsch, R.D., 2005. Metamorphosis of two amphibian species after chronic cadmium exposure in outdoor aquatic mesocosms. Environ Toxicol Chem 24, 1994–2001. https://doi.org/10.1897/04-568R.1.

[19] Sun, N., Wang, H., Ju, Z., Zhao, H., 2018. Effects of chronic cadmium exposure on metamorphosis, skeletal development, and thyroid endocrine disruption in Chinese toad *Bufo gargarizans* tadpoles. Environ Toxicol Chem 37, 213–223. https://doi.org/10.1002/etc.3947.

[20] Snodgrass, J.W., Hopkins, W.A., Roe, J.H., 2003. Relationships among developmental stage, metamorphic timing, and concentrations of elements in Bullfrogs (*Rana catesbeiana*). Environ Toxicol Chem 22, 1597–1604. https://doi.org/10.1002/etc.5620220724.

[21] Unrine, J.M., Hopkins, W.A., Romanek, C.S., Jackson, B.P., 2007. Bioaccumulation of trace elements in omnivorous amphibian larvae: implications for amphibian health and contaminant transport. Environ Pollut 149, 182–192. https://doi.org/10.1016/j.envpol.2007.01.039.

[22] Cresswell, T., Metian, M., Golding, L.A., Wood, M.D., 2017. Aquatic live animal radiotracing studies for ecotoxicological applications: addressing fundamental methodological deficiencies. J Environ Radio 178–179 453–460. https://doi.org/10.1016/j.jenvrad.2017.05.017.

[23] Lanctôt, C., Cresswell, T., Melvin, S.D., 2017. Uptake and tissue distributions of cadmium, selenium and zinc in striped marsh frog tadpoles exposed during early post-embryonic development. Ecotoxicol Environ Saf 144, 291–299. https://doi.org/10.1016/j.ecoenv.2017.06.047.

[24] Gosner, K.L., 1960. A simplified table for staging Anuran embryos and larvae with notes on identification. Herpetologica 16, 183–190.

[25] US EPA, 2002. Short-term methods for estimating the chronic toxicity of effluents and receiving waters to freshwater organisms, EPA-821-R-02–013. Washington, DC. https://doi.org/10.1017/CBO9781107415324.004.

[26] Lanctôt, C., Cresswell, T., Lombi, E., Bennett, W., 2021. Synchrotron-based imaging reveals the fate of selenium in striped marsh frog tadpoles. Environ Sci Technol 55 (17), 11848–11858. https://doi.org/10.1021/acs.est.1c02028.

[27] Hervé-Fernández, P., Houlbrèque, F., Boisson, F., Mulsow, S., Teyssié, J.L., Oberhaënsli, F., et al., 2010. Cadmium bioaccumulation and retention kinetics in the Chilean blue mussel *Mytilus chilensis*: seawater and food exposure pathways. Aquat Toxicol 99, 448–456. https://doi.org/10.1016/j.aquatox.2010.06.004.

[28] Lee, B.G., Lee, J.S., Luoma, S.N., 2006. Comparison of selenium bioaccumulation in the clams *Corbicula fluminea* and *Potamocorbula amurensis*: A bioenergetic modeling approach. Environ Toxicol Chem 25, 1933–1940. https://doi.org/10.1897/05-540R.1.

[29] Creighton, N., Twining, J., 2010. Bioaccumulation from food and water of cadmium, selenium and zinc in an estuarine fish, *Ambassis jacksoniensis*. Mar Pollut Bull 60, 1815–1821. https://doi.org/10.1016/j.marpolbul.2010.05.025.

[30] Altig, R., McDearman, W., 1975. Percent assimilation and clearance times of five anuran tadpoles. Herpetologica 31, 67–69.

[31] Pryor, G.S., 2003. Growth rates and digestive abilities of bullfrog tadpoles (*Rana catesbeiana*) fed algal diets. J Herpetol 37, 560–566. https://doi.org/10.1670/153-02N.

[32] Heyes, A., Rowe, C.L., Conrad, P., 2014. Differential patterns of accumulation and retention of dietary trace elements associated with coal ash during larval development and metamorphosis of an amphibian. Arch Environ Contam Toxicol 66, 78–85. https://doi.org/10.1007/s00244-013-9957-6.

[33] Roe, J.H., Hopkins, W.A., Jackson, B.P., 2005. Species- and stage-specific differences in trace element tissue concentrations in amphibians: implications for the disposal of coal-combustion wastes. Environ Pollut 136, 353–363. https://doi.org/10.1016/j.envpol.2004.11.019.

[34] Snodgrass, J.W., Hopkins, W.A., Broughton, J., Gwinn, D., Baionno, J.A., Burger, J., 2004. Species-specific responses of developing anurans to coal combustion wastes. Aquat Toxicol 66, 171–182. https://doi.org/10.1016/j.aquatox.2003.09.002.

[35] Fritz, K.A., Whiles, M.R., 2018. Amphibian-mediated nutrient fluxes across aquatic–terrestrial boundaries of temporary wetlands. Freshw Biol 63, 1250–1259. https://doi.org/10.1111/FWB.13130.

[36] Herkovits, J., Cardellini, P., Pavanati, C., Pérez-Coll, C.S., 1998. Cadmium uptake and bioaccumulation in *Xenopus laevis* embryos at different developmental stages. Ecotoxicol Environ Saf 39, 21–26. https://doi.org/10.1006/eesa.1997.1586.

[37] Kirschman, L.J., McCue, M.D., Boyles, J.G., Warne, R.W., 2017. Exogenous stress hormones alter energetic and nutrient costs of development and metamorphosis. J Exp Biol 220, 3391–3397. https://doi.org/10.1242/jeb.164830.

[38] Pfab, F., DiRenzo, G.V., Gershman, A., Briggs, C.J., Nisbet, R.M., 2020. Energy budgets for tadpoles approaching metamorphosis. Ecol Model 436, 109261. https://doi.org/10.1016/j.ecolmodel.2020.109261.

[39] Hourdry, J., L'Hermite, A., Ferrand, R., 1996. Changes in the digestive tract and feeding behavior of anuran amphibians during metamorphosis. Physiol Zool 69, 219–251. https://doi.org/10.1086/physzool.69.2.30164181.

[40] Leney, J.L., Drouillard, K.G., Haffner, G.D., 2006. Metamorphosis increases biotransformation of polychlorinated biphenyls: a comparative study of polychlorinated biphenyl metabolism in green frogs (*Rana clamitans*) and leopard frogs (*Rana pipiens*) at various life stages. Environ Toxicol Chem 25, 2971–2980. https://doi.org/10.1897/05-561R1.1.

[41] Ishizuya-Oka, A., Hasebe, T., Shi, Y.B., 2010. Apoptosis in amphibian organs during metamorphosis. Apoptosis 15, 350–364. https://doi.org/10.1007/s10495-009-0422-y.

[42] Shi, Y.B., Fu, L., Hsia, S.C.V., Tomita, A., Buchholz, D., 2001. Thyroid hormone regulation of apoptotic tissue remodeling during anuran metamorphosis. Cell Res 11, 245–252. https://doi.org/10.1038/sj.cr.7290093.

[43] Yoshizato, K., 1989. Biochemistry and cell biology of amphibian metamorphosis with a special emphasis on the mechanism of removal of larval organs. Int Rev Cytol 119, 97–149. https://doi.org/10.1016/S0074-7696(08)60650-6.

[44] Alquezar, R., Markich, S.J., Twining, J.R., 2008. Comparative accumulation of 109Cd and 75Se from water and food by an estuarine fish (*Tetractenos glaber*). J Environ Radioact 99, 167–180. https://doi.org/10.1016/j.jenvrad.2007.07.012.

[45] Pavlaki, M.D., Morgado, R.G., Ferreira, V., Rocha, R.J.M., Soares, A.M.V.M., Calado, R., et al., 2021. Cadmium accumulation and kinetics in *Solea senegalensis* tissues under dietary and water exposure and the link to human health. Water (Switz) 13, 522. https://doi.org/10.3390/w13040522.

[46] Handy, R.D., 1992. The assessment of episodic metal pollution. I. Uses and limitations of tissue contaminant analysis in rainbow trout (*Oncorhynchus mykiss*) after short waterborne exposure to cadmium or copper. Arch Environ Contam Toxicol 22, 74–81. https://doi.org/10.1007/BF00213304.

[47] Szebedinszky, C.S., McGeer, J.C., McDonald, D.G., Wood, C.M., 2001. Effects of chronic Cd exposure via the diet or water on internal organ-specific distribution and subsequent gill Cd uptake kinetics in juvenile rainbow trout (*Oncorhynchus mykiss*). Environ Toxicol Chem 20, 597–607. https://doi.org/10.1002/etc.5620200320.

[48] Pryor, G.S., Bjorndal, K.A., 2005. Symbiotic fermentation, digesta passage, and gastrointestinal morphology in bullfrog tadpoles (*Rana catesbeiana*). Physiol Biochem Zool 78, 201–215. https://doi.org/10.1086/427050.

[49] Kalman, J., Riba, I., Ángel DelValls, T., Blasco, J., 2010. Comparative toxicity of cadmium in the commercial fish species *Sparus aurata* and *Solea senegalensis*. Ecotoxicol Environ Saf 73, 306–311. https://doi.org/10.1016/j.ecoenv.2009.10.013.

[50] Kraal, M.H., Kraak, M.H.S., De Groot, C.J., Davids, C., 1995. Uptake and tissue distribution of dietary and aqueous cadmium by carp (*Cyprinus carpio*). Ecotoxicol Environ Saf 31, 179–183. https://doi.org/10.1006/eesa.1995.1060.

[51] Pelgrom, S.M.G.J., Lamers, L.P.M., Lock, R.A.C., Balm, P.H.M., Bonga, S.E.W., 1995. Interactions between copper and cadmium modify metal organ distribution in mature tilapia, *Oreochromis mossambicus*. Environ Pollut 90, 415–423. https://doi.org/10.1016/0269-7491(95)00022-J.

[52] Ishizuya-Oka, A., 2011. Amphibian organ remodeling during metamorphosis: insight into thyroid hormone-induced apoptosis. Dev Growth Differ 53, 202–212. https://doi.org/10.1111/J.1440-169X.2010.01222.X.

[53] Shi, Yun-Bo, Ishizuya-Oka, A., 1996. Biphasic intestinal development in amphibians: embryogenesis and remodeling during metamorphosis. Curr Top Dev Biol 32, 205–235. https://doi.org/10.1016/s0070-2153(08)60429-9.

[54] Mu, D., Meng, J., Bo, X., Wu, M., Xiao, H., Wang, H., 2018. The effect of cadmium exposure on diversity of intestinal microbial community of *Rana chensinensis* tadpoles. https://doi.org/10.1016/j.ecoenv.2018.02.022.

[55] Ya, J., Li, X., Wang, L., Kou, H., Wang, H., Zhao, H., 2020. The effects of chronic cadmium exposure on the gut of *Bufo gargarizans* larvae at metamorphic climax: histopathological impairments, microbiota changes and intestinal remodeling disruption. Ecotoxicol Environ Saf 195, 110523. https://doi.org/10.1016/j.ecoenv.2020.110523.

[56] Atkinson, B.G., Just, J.J., 1975. Biochemical and histological changes in the respiratory system of *Rana catesbeiana* larvae during normal and induced metamorphosis. Dev Biol 45, 151–165. https://doi.org/10.1016/0012-1606(75)90248-1.

[57] Izutsu, Y., Kaiho, M., Yoshizato, K., 1993. Different distribution of epidermal basal cells in the anuran larval skin correlates with the skin's region-specific fate at metamorphosis. J Exp Zool 267, 605–615. https://doi.org/10.1002/jez.1402670608.

[58] Schreiber, A.M., Brown, D.D., 2003. Tadpole skin dies autonomously in response to thyroid hormone at metamorphosis. Proc Natl Acad Sci USA 100, 1769–1774. https://doi.org/10.1073/pnas.252774999.

[59] Simoncelli, F., Belia, S., Di Rosa, I., Paracucchi, R., Rossi, R., La Porta, G., et al., 2015. Short-term cadmium exposure induces stress responses in frog (*Pelophylax bergeri*) skin organ culture. Ecotoxicol Environ Saf 122, 221–229. https://doi.org/10.1016/j.ecoenv.2015.08.001.

[60] Flament, S., Kuntz, S., Chesnel, A., Grillier-Vuissoz, I., Tankozic, C., Penrad-Mobayed, M., et al., 2003. Effect of cadmium on gonadogenesis and metamorphosis in *Pleurodeles waltl* (urodele amphibian). Aquat Toxicol 64, 143–153. https://doi.org/10.1016/S0166-445X(03)00042-0.

[61] De Smet, H., De Wachter, B., Lobinski, R., Blust, R., 2001. Dynamics of (Cd,Zn)-metallothioneins in gills, liver and kidney of common carp *Cyprinus carpio* during cadmium exposure. Aquat Toxicol 52, 269–281.

[62] Hogstrand, C., Haux, C., 1991. Binding and detoxification of heavy metals in lower vertebrates with reference to metallothionein. Comparative Biochemistry and

Physiology. Part C, Comparative. https://doi.org/10.1016/0742–8413(91)90140-O.

[63] Mouchet, F., Teaniniuraitemoana, V., Baudrimont, M., Daffe, G., Gauthier, L., Gonzalez, P., 2015. Recovery capabilities of *Xenopus laevis* after exposure to cadmium and zinc. Chemosphere 139, 117–125. https://doi.org/10.1016/j.chemosphere.2015.05.103.

[64] Ya, J., Xu, Y., Wang, G., Zhao, H., 2021. Cadmium induced skeletal underdevelopment, liver cell apoptosis and hepatic energy metabolism disorder in *Bufo gargarizans* larvae by disrupting thyroid hormone signaling. Ecotoxicol Environ Saf 211, 111958. https://doi.org/10.1016/j.ecoenv.2021.111957.

[65] Jeffree, R.A., Warnau, M., Teyssié, J.-L., Markich, S.J., 2006. Comparison of the bioaccumulation from seawater and depuration of heavy metals and radionuclides in the spotted dogfish *Scyliorhinus canicula* (Chondrichthys) and the turbot *Psetta maxima* (Actinopterygii: Teleostei). Sci Total Environ 368, 839–852. https://doi.org/10.1016/j.scitotenv.2006.03.026.

[66] Engström, B., Nordberg, G.F., 1979. Dose dependence of gastrointestinal absorption and biological half-time of cadmium in mice. Toxicology 13, 215–222. https://doi.org/10.1016/S0300-483X(79)80025-6.

[67] Harrison, S.E., Klaverkamp, J.F., 1989. Uptake, elimination and tissue distribution of dietary and aqueous cadmium by rainbow trout (*Salmo gairdneri* Richardson) and lake whitefish (*Coregonus clupeaformis* Mitchill). Environ Toxicol Chem 8, 87–97. https://doi.org/10.1002/etc.5620080110.

[68] Ma, Y., Ran, D., Shi, X., Zhao, H., Liu, Z., 2021. Cadmium toxicity: A role in bone cell function and teeth development. https://doi.org/10.1016/j.scitotenv.2020.144646.

[69] Bawden, J.W., Hammarstrom, L.E., 1975. Distribution of cadmium in developing teeth and bone of young rats. Eur J Oral Sci 83, 179–186. https://doi.org/10.1111/j.1600-0722.1975.tb01196.x.

[70] Hinkle, P.M., Kinsella, P.A., Osterhoudt, K.C., 1987. Cadmium uptake and toxicity via voltage-sensitive calcium channels. J Biol Chem 262, 16333–16337. https://doi.org/10.1016/s0021-9258(18)49259-9.

[71] Teng, Y., Ren, C., Chen, X., Shen, Y., Zhang, Z., Chai, L., et al., 2022. Effects of cadmium exposure on thyroid gland and endochondral ossification in *Rana zhenhaiensis*. Environ Toxicol Pharm 92, 103860. https://doi.org/10.1016/j.etap.2022.103860.

[72] Chen, A., Deng, H., Song, X., Liu, X., Chai, L., 2022. Effects of separate and combined exposure of cadmium and lead on the endochondral ossification in *Bufo gargarizans*. Environ Toxicol Chem 41, 1228–1245. https://doi.org/10.1002/etc.5296.

[73] Schlenk, D., de Almeida, E.A., 2024. Toxicokinetic pathways of environmental contaminants in amphibian tadpoles, in: Toxicology of Amphibian Tadpoles. CRC Press, pp. 36–62. https://doi.org/10.1201/9781003091394–3.

[74] Schreiber, A.M., Cai, L., Brown, D.D., 2005. Remodeling of the intestine during metamorphosis of *Xenopus laevis*. Proc Natl Acad Sci USA 102, 3720–3725. https://doi.org/10.1073/pnas.0409868102.

[75] Howes, N.H., 1947. The skin of the tadpole of the common toad, *Bufo bufo bufo* (L.), during metamorphosis. Proc Zool Soc Lond 116, 602–610. https://doi.org/10.1111/j.1096-3642.1947.tb00138.x.

[76] Minnich, B., Bartel, H., Lametschwandtner, A., 2002. How a highly complex three-dimensional network of blood vessels regresses: The gill blood vascular system of tadpoles of *Xenopus* during metamorphosis. A SEM study on microvascular corrosion casts. Micro Res 64, 425–437. https://doi.org/10.1006/mvre.2002.2422.

[77] Brown, G.W., Brown, W.R., Cohen, P.P., 1959. Comparative biochemistry of urea synthesis. II Levels of urea cycle enzymes in metamorphosing *Rana catesbeiana* tadpoles. J Biol Chem 234, 1775–1780. https://doi.org/10.1016/s0021-9258(18)69924-7.

[78] Egea-Serrano, A., Relyea, R.A., Tejedo, M., Torralva, M., 2012. Understanding of the impact of chemicals on amphibians: a meta-analytic review. Ecol Evol 2, 1382–1397. https://doi.org/10.1002/ece3.249.

[79] Luedtke, J.A., Chanson, J., Neam, K., Hobin, L., Maciel, A.O., Catenazzi, A., et al., 2023. Ongoing declines for the world's amphibians in the face of emerging threats. Nature 622, 308–314. https://doi.org/10.1038/s41586-023-06578-4.

[80] Grott, S.C., Rutkoski, C.F., de Almeida, E.A., 2024. The importance of tadpole staging in ecotoxicological studies, in: Toxicology of Amphibian Tadpoles. CRC Press, pp. 27–35. https://doi.org/10.1201/9781003091394–2.

[81] Wang, W.X., Tan, Q.G., 2019. Applications of dynamic models in predicting the bioaccumulation, transport and toxicity of trace metals in aquatic organisms. Environ Pollut 252, 1561–1573. https://doi.org/10.1016/j.envpol.2019.06.043.

[82] Cresswell, T., Smith, R.E.W., Nugegoda, D., Simpson, S.L., 2013. Challenges with tracing the fate and speciation of mine-derived metals in turbid river systems: implications for bioavailability. https://doi.org/10.1007/s11356–013-2066–2.